Sulfobetaine ionic liquid crystals based on strong acids: phase behavior and electrochemistry

Alyna Lange[1,*], Nadia Kapernaum[2], Zaneta Wojnarowska[3], Lea Holtzheimer[1], Stefan Mies[1], Vance Williams[4], Frank Gießelmann[2], Andreas Taubert[1,*]

Synthesis and analytical data of the ZIs

All ZIs were synthesized following a previously published protocol.[1,2] The amine was put into a two-neck round-bottom flask and stirred with a magnetic stir bar at room temperature. An equimolar amount of 1,4-butanesultone was slowly added via a syringe. After complete addition, the mixture was heated to 60 °C. When the formation of a white solid was observed, acetone was added and the reaction mixture was left to reflux for several days until sufficient amounts of precipitate were achieved. Upon cooling to room temperature the solid was filtered, washed with cold acetone (3x) and dried via rotary evaporator.

DmC$_{10}$S: yield: 89.5 %; ESI-MS: 322.240 g/mol (molecular mass + H$^+$); ^{1}H NMR (400 MHz, D$_2$O): δ [ppm]: 0.87 (m, 3 H) 1.21 - 1.43 (m, 14 H) 1.66 - 1.97 (m, 6 H) 2.92 (t, 2 H) 3.06 (s, 6 H) 3.21 - 3.38 (m, 4 H).

DmC$_{12}$S: yield: 91.5 %; ESI-MS: 350.273 g/mol (molecular mass + H$^+$); ^{1}H NMR (400 MHz, D$_2$O): δ [ppm]: 0.91 (t, 3 H) 1.23 - 1.56 (m, 18 H) 1.69 - 2.03 (m, 6 H) 2.95 (t, 2 H) 3.13 (s, 6 H) 3.29 - 3.46 (m, 4 H).

DmC$_{14}$S: yield: 86.4 %; ESI-MS: 378.306 g/mol (molecular mass + H$^+$); ^{1}H NMR (400 MHz, D$_2$O): δ [ppm]: 1.03 - 1.17 (m, 3 H) 1.31 - 1.77 (m, 22 H) 1.87 - 2.28 (m, 6 H) 3.18 (t, 2 H) 3.37 (s, 6 H) 3.49 - 3.74 (m, 4 H).

DmC$_{16}$S: yield: 74.7 %; ESI-MS: 406.336 g/mol (molecular mass + H$^+$); ^{1}H NMR (400 MHz, D$_2$O): δ [ppm]: 0.95 - 1.09 (m, 3 H) 1.23 - 1.77 (m, 25 H) 1.78 - 2.18 (m, 6 H) 3.06 - 3.12 (m, 2 H) 3.27 (s, 6 H) 3.40 - 3.64 (m, 4 H).

NMR-data of the ILCs

DmC$_{10}$S MeSO$_3$: ^{1}H NMR (400 MHz, D$_2$O): δ [ppm]: 0.73 - 0.94 (m, 3 H) 1.18 - 1.41 (m, 14 H) 1.60 - 1.93 (m, 6 H) 2.74 (s, 3 H) 2.89 (t, *J*=8.00 Hz, 1 H) 3.03 (s, 1 H) 3.17 - 3.33 (m, 4 H); ^{13}C NMR (101 MHz, D$_2$O): δ [ppm]: 13.65 (s, 1 C) 20.92 (s, 1 C) 21.21 (s, 1 C) 21.96 (s, 1 C) 22.30 (s, 1 C) 25.70 (s, 1 C) 28.51 (s, 1 C) 28.86 (s, 1 C) 28.90 (s, 1 C) 29.00 (s, 1 C) 31.51 (s, 1 C) 38.41 (s, 1 C) 50.03 (s, 1 C) 50.71 (br s, 1 C) 63.09 (br s, 1 C) 63.95 (s, 1 C).

DmC$_{12}$S MeSO$_3$: ^{1}H NMR (400 MHz, D$_2$O): δ [ppm]: 0.76 - 0.93 (m, 3 H) 1.18 - 1.41 (m, 18 H) 1.61 - 1.98 (m, 6 H) 2.73 (s, 3 H) 2.85 (t, *J*=7.38 Hz, 2 H) 3.04 (s, 6 H) 3.15 - 3.39 (m, 4 H); ^{13}C NMR (101 MHz, D$_2$O): δ [ppm]: 13.86 (s, 1 C) 21.00 (s, 1 C) 21.37 (s, 1 C) 22.23 (s, 1 C) 22.62 (s, 1 C) 26.10 (s, 1 C) 29.06 (s, 1 C) 29.44 (s, 1 C) 29.55 (s, 1 C) 29.66 (s, 1 C) 29.76 (s, 1 C) 29.80 (s, 1 C) 31.94 (s, 1 C) 38.42 (s, 1 C) 50.10 (s, 1 C) 50.87 (s, 1 C) 63.00 (s, 1 C) 63.66 (s, 1 C).

DmC$_{14}$S MeSO$_3$: ^{1}H NMR (400 MHz, D_2O): δ [ppm]: 0.67 – 0.97 (m, 3 H) 1.13 - 1.40 (m, 22 H) 1.58 - 1.94 (m, 6 H) 2.72 (s, 3 H) 2.79 - 2.90 (m, 2 H) 3.04 (s, 6 H) 3.17 - 3.37 (m, 4 H); ^{13}C NMR (101 MHz, D_2O): δ [ppm]: 13.89 (s, 1 C) 21.04 (s, 1 C) 21.42 (s, 1 C) 22.32 (s, 1 C) 22.67 (s, 1 C) 26.21 (s, 1 C) 29.20 (s, 1 C) 29.56 (s, 1 C) 29.73 (s, 1 C) 29.85 (s, 1 C) 29.90 (s, 1 C) 30.01 (s, 1 C) 32.02 (s, 1 C) 38.43 (s, 1 C) 42.66 (s, 1 C) 50.13 (s, 1 C) 50.90 (s, 1 C) 63.06 (s, 1 C) 63.69 (s, 1 C).

DmC$_{16}$S MeSO$_3$: ^{1}H NMR (400 MHz, D_2O): δ [ppm]: 0.86 - 0.97 (m, 3 H) 1.24 - 1.53 (m, 26 H) 1.67 - 2.07 (m, 6 H) 2.83 (s, 1 H) 2.95 (t, *J*=7.30 Hz, 2 H) 3.16 (s, 6 H) 3.30 - 3.48 (m, 4 H); ^{13}C NMR (101 MHz, D_2O): δ [ppm]: 13.95 (s, 1 C) 21.16 (s, 1 C) 21.52 (s, 1 C) 22.45 (s, 1 C) 22.76 (s, 1 C) 26.34 (s, 1 C) 29.34 (s, 1 C) 29.67 (s, 1 C) 29.86 (s, 1 C) 30.02 (s, 1 C) 30.15 (br s, 1 C) 30.18 (s, 1 C) 30.22 (s, 1 C) 32.12 (s, 1 C) 38.55 (s, 1 C) 50.24 (s, 1 C) 50.82 (s, 1 C) 63.36 (s, 1 C) 63.93 (s, 1 C).

DmC$_{10}$S HSO$_4$: ^{1}H NMR (400 MHz, D_2O): δ [ppm]: 0.73 - 0.90 (m, 3 H) 1.09 - 1.46 (m, 14 H) 1.54 - 2.00 (m, 6 H) 2.86 (t, *J*=7.50 Hz, 2 H) 3.00 (s, 6 H) 3.13 - 3.33 (m, 4 H) 3.65 (s, 1 H); ^{13}C NMR (101 MHz, D_2O): δ [ppm]: 13.73 (s, 1 C) 20.94 (s, 1 C) 21.24 (s, 1 C) 22.03 (s, 1 C) 22.39 (s, 1 C) 25.81 (s, 1 C) 28.66 (s, 1 C) 29.00 (s, 1 C) 29.08 (s, 1 C) 29.16 (s, 1 C) 31.63 (s, 1 C) 50.04 (s, 1 C) 50.71 (s, 1 C) 63.03 (s, 1 C) 63.86 (s, 1 C).

DmC$_{12}$S HSO$_4$: ^{1}H NMR (400 MHz, D_2O): δ [ppm]: 0.72 - 0.97 (m, 3 H) 1.13 - 1.44 (m, 18 H) 1.61 - 1.97 (m, 6 H) 2.85 (t, *J*=7.80 Hz, 1 H) 3.04 (s, 6 H) 3.15 - 3.44 (m, 4 H) 3.66 (s, 1 H); ^{13}C NMR (101 MHz, D_2O): δ [ppm]: 13.86 (s, 1 C) 21.00 (s, 1 C) 21.37 (s, 1 C) 22.23 (s, 1 C) 22.61 (s, 1 C) 26.09 (s, 1 C) 29.06 (s, 1 C) 29.43 (s, 1 C) 29.55 (s, 1 C) 29.65 (s, 1 C) 29.75 (s, 1 C) 29.79 (s, 1 C) 31.93 (s, 1 C) 50.09 (s, 1 C) 50.85 (s, 1 C) 62.99 (s, 1 C) 63.65 (s, 1 C).

DmC$_{14}$S HSO$_4$: ^{1}H NMR (400 MHz, D_2O): δ [ppm]: 0.76 - 0.88 (m, 3 H) 1.11 - 1.44 (m, 22 H) 1.58 - 1.95 (m, 6 H) 2.83 (t, *J*=7.50 Hz, 2 H) 3.03 (s, 6 H) 3.15 - 3.36 (m, 4 H); ^{13}C NMR (101 MHz, D_2O): δ [ppm]: 13.86 (s, 1 C) 21.01 (s, 1 C) 21.39 (s, 1 C) 22.28 (s, 1 C) 22.65 (s, 1 C) 26.17 (s, 1 C) 29.17 (s, 1 C) 29.53 (s, 1 C) 29.70 (s, 1 C) 29.82 (s, 1 C) 29.87 (s, 1 C) 29.98 (s, 1 C) 31.99 (s, 1 C) 50.09 (s, 1 C) 50.87 (s, 1 C) 62.99 (s, 1 C) 63.61 (s, 1 C).

DmC$_{16}$S HSO$_4$: ^{1}H NMR (400 MHz, D_2O): δ [ppm]: 0.75 - 0.90 (m, 3 H) 1.14 - 1.45 (m, 26 H) 1.60 - 1.95 (m, 6 H) 2.84 (t, *J*=7.25 Hz, 2 H) 3.06 (s, 6 H) 3.16 - 3.38 (m, 4 H) 3.64 (s, 1 H); ^{13}C NMR (101 MHz, D_2O): δ [ppm]: 13.86 (s, 1 C) 21.02 (s, 1 C) 21.43 (s, 1 C) 22.31 (s, 1 C) 22.67 (s, 1 C) 26.21 (s, 1 C) 29.23 (s, 1 C) 29.57 (s, 1 C) 29.76 (s, 1 C) 29.92 (s, 1 C) 30.04 (s, 1 C) 30.09 (s, 1 C) 30.12 (s, 1 C) 32.03 (s, 1 C) 50.11 (s, 1 C) 50.85 (s, 1 C) 63.03 (s, 1 C) 63.62 (s, 1 C).

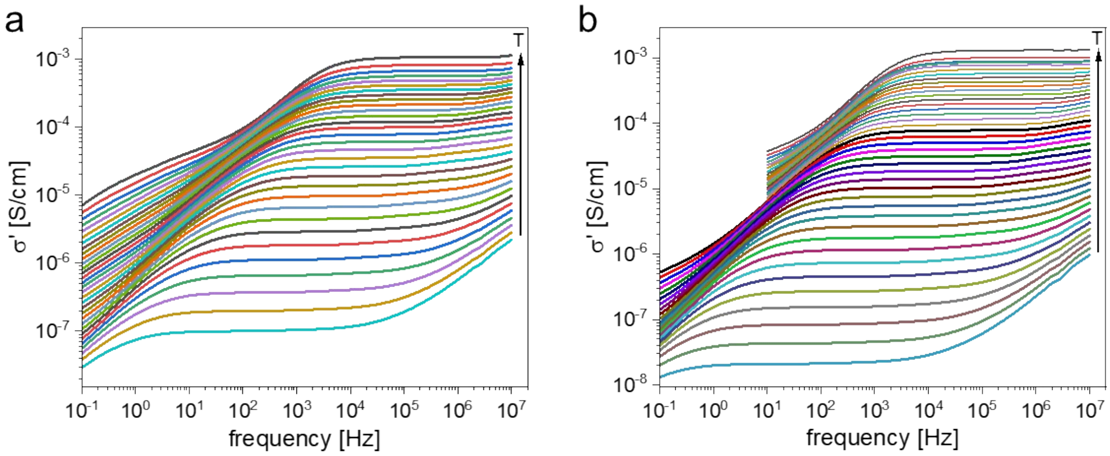

Figure S1: Representative plots of the real part of complex conductivity vs. frequency at different temperatures for **a)** $DmC_{10}S\ HSO_4$, and **b)** $DmC_{12}S\ HSO_4$. Conductivity values were taken from the frequency-independent plateau regions.

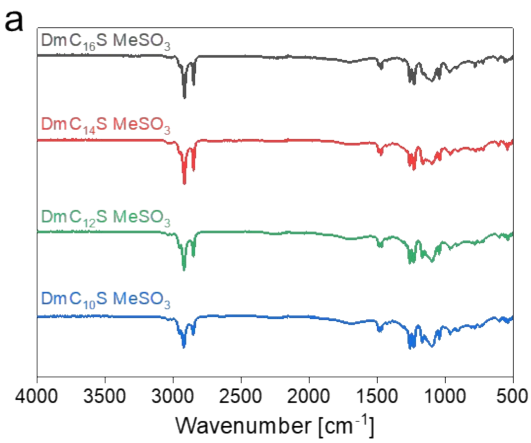

Figure S2: IR spectra of **a)** mesylate based ILCs, and **b)** hydrogen sulfate based ILCs.

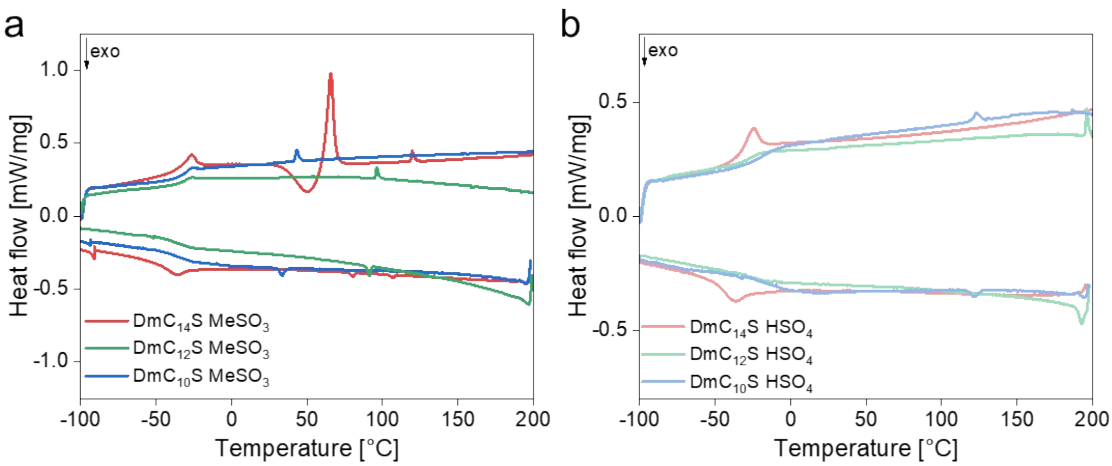

Figure S3: 2^{nd} heating and cooling DSC runs of **a)** short-chained mesylate based ILCs, and **b)** hydrogen sulfate based ILCs.

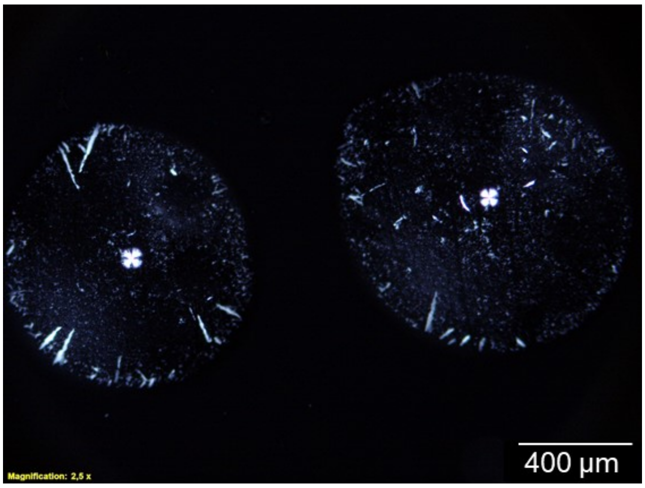

Figure S4: POM image of $DmC_{14}S$ $MeSO_3$ at 90 °C upon cooling.

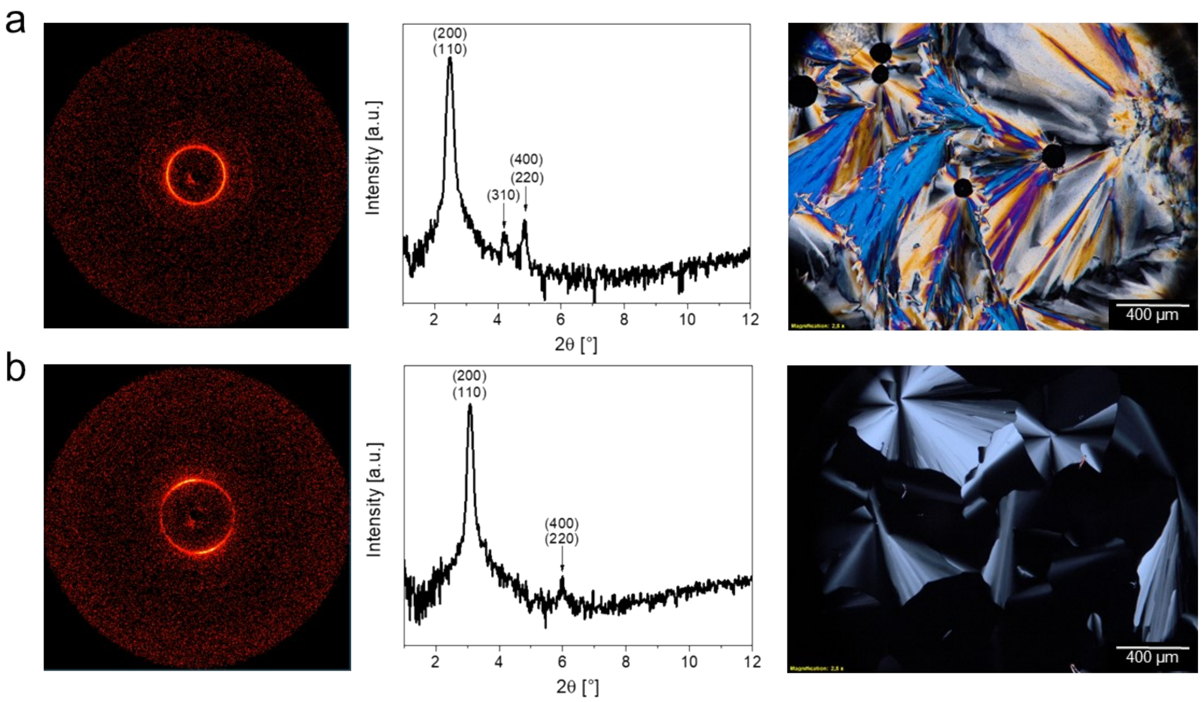

Figure S5: 2D diffraction patterns, integrated diffractograms and POM images of **a)** $DmC_{14}S$ HSO_4 at 75 °C, and **b)** $DmC_{10}S$ HSO_4 at 25 °C.

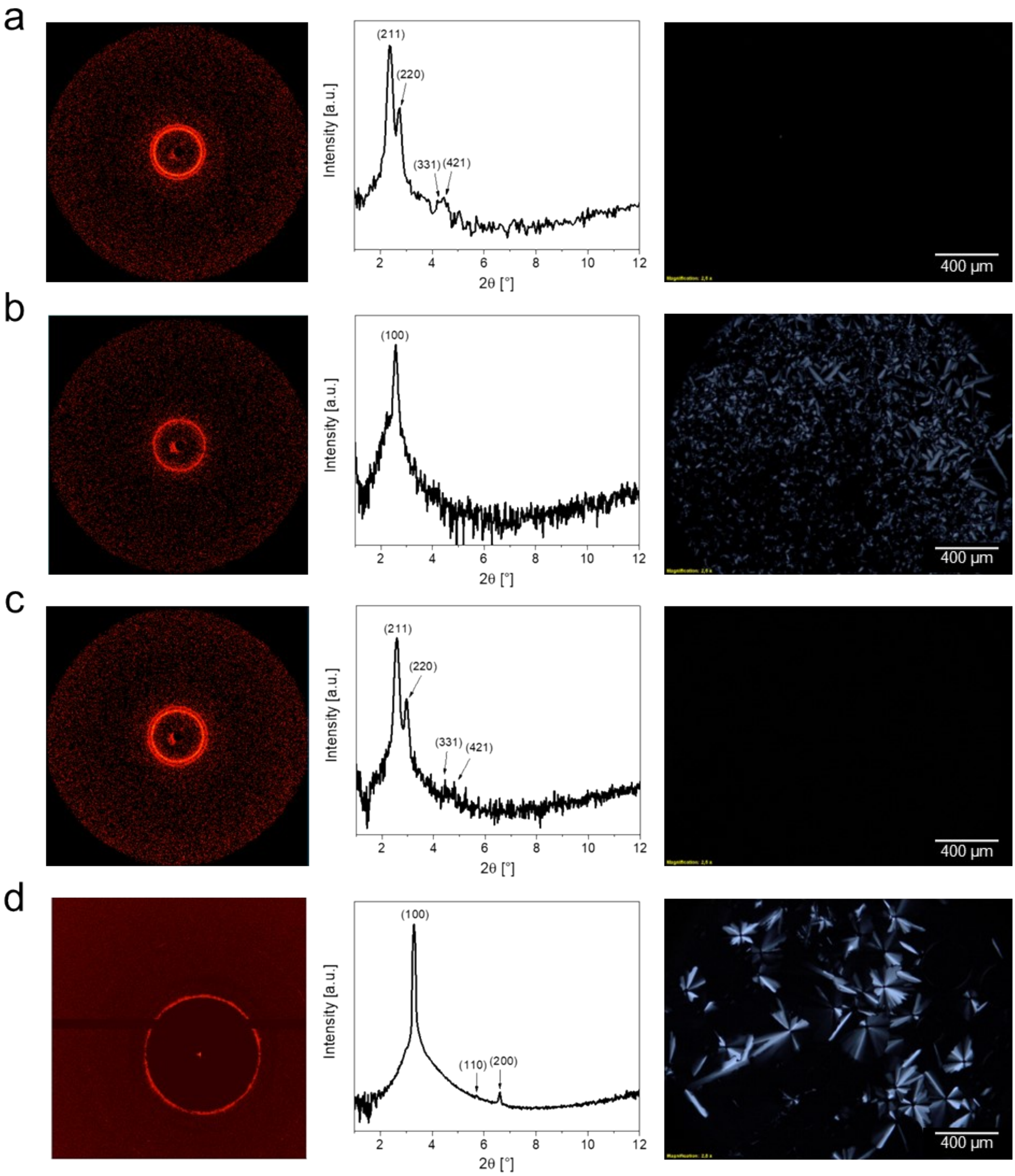

Figure S6: 2D diffraction patterns, integrated diffractograms and POM images of **a)** $DmC_{16}S$ $MeSO_3$ at 95 °C, **b)** $DmC_{16}S$ $MeSO_3$ at 170 °C, **c)** $DmC_{14}S$ $MeSO_3$ at 75 °C, and **d)** $DmC_{10}S$ $MeSO_3$ at 20 °C.

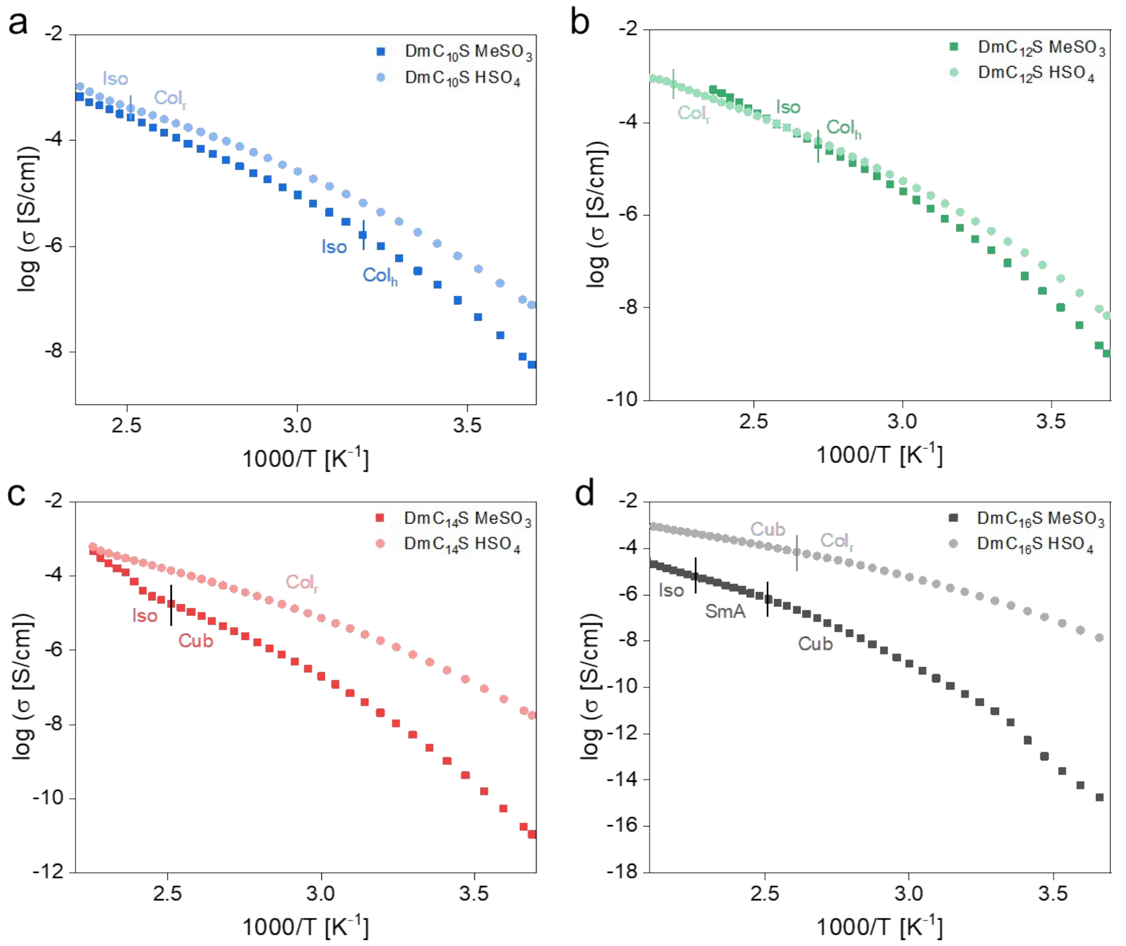

Figure S7: Comparisons of ionic conductivities for a) $DmC_{10}S$ ILCs, b) $DmC_{12}S$ ILCs, c) $DmC_{14}S$ ILCs, and d) $DmC_{16}S$ ILCs. The vertical lines are drawn at phase transition temperatures.

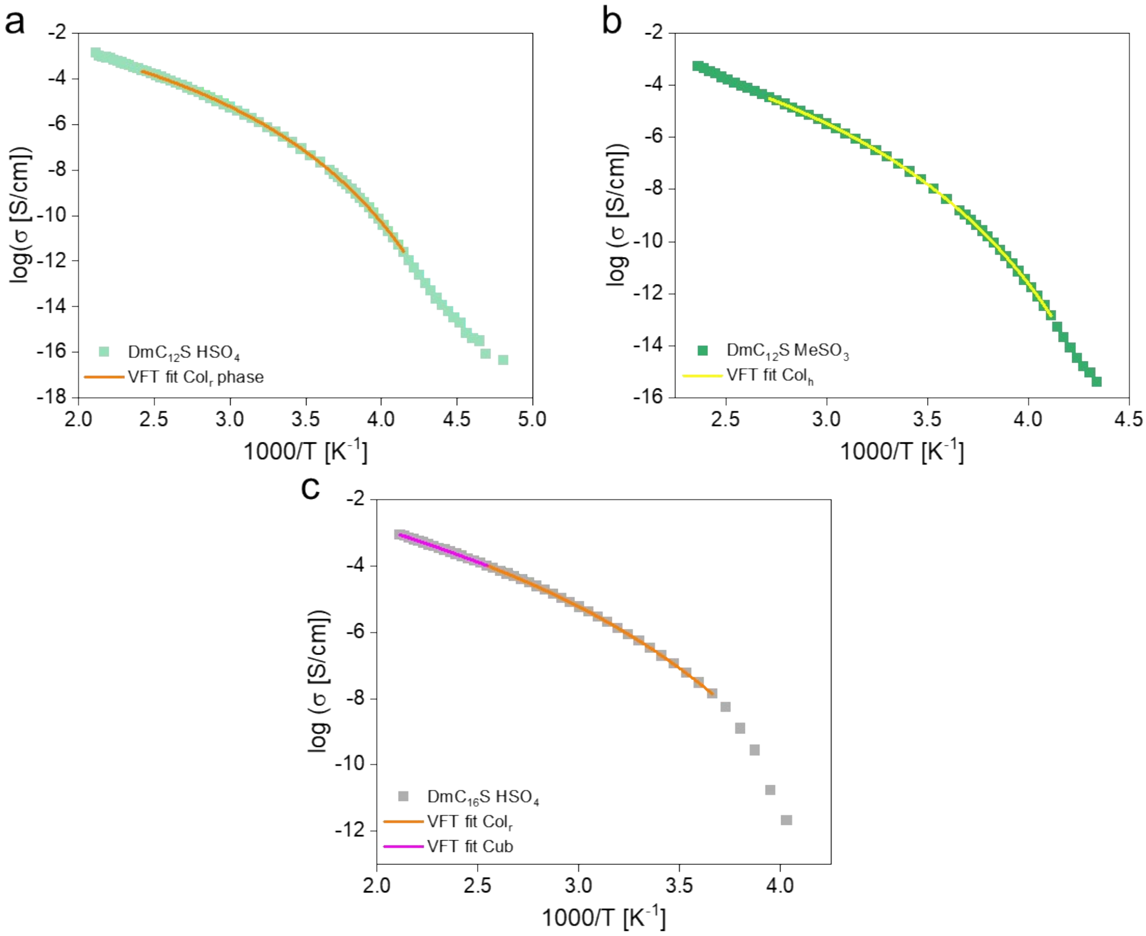

Figure S8: Representative VFT fits for a) $DmC_{12}S\ HSO_4$, b) $DmC_{12}S\ MeSO_3$, and c) $DmC_{16}S\ HSO_4$ with two VFT fits.

References:

1) Zehbe, K.; Lange, A.; Taubert, A. Stereolithography Provides Access to 3D Printed Ionogels with High Ionic Conductivity. *Energy Fuels* **2019**, *33*, 12885–12893.

2) Delahaye, E.; Göbel, R.; Löbbicke, R.; Guillot, R.; Sieber, C.; Taubert, A. Silica ionogels for proton transport. *J. Mater. Chem.* **2012**, *22*, 17140.

3) Taubert, A.; Löbbicke, R.; Kirchner, B.; Leroux, F. First examples of organosilica-based ionogels: synthesis and electrochemical behavior. *Beilstein journal of nanotechnology* **2017**, *8*, 736–751.